№ 1 (5), 2022

УДК 621.313.333

M. Semeniuk
Lviv Polytechnic National University,
Department of Electromechatronics and Computerized Electromechanical Systems,
mykola.b.semeniuk@lpnu.ua

A. Kutsyk
Lviv Polytechnic National University,
Department of Electromechatronics and Computerized Electromechanical Systems,
andrii.s.kutsyk@lpnu.ua

Grzegorz Podskarbi
Rzeszow University of Technology,
Faculty of Electrical and Computer Engineering,
g.podskarbi@prz.edu.pl

DUAL-MOTOR INDUCTION FREQUENCY-REGULATED ELECTRIC DRIVE WITH IMPROVED ELECTROMAGNETIC AND ELECTROMECHANICAL COMPATIBILITY

http://doi.org/10.23939/sepes2022.01.024

Dual-motor induction frequency-regulated electric drive is used as an alternative to single-motor electric drive in case where there are difficulties in implementing an individual drive which are associated with the mechanical-transmission implementation. Dual-motor electric drive provides movement of traction mechanisms, working bodies of electric vehicles. Single- or dual-voltage source inverters with pulse-width modulation are used to power two induction motors. The disadvantage of such voltage source inverters is that the AC voltage is formed as a high-frequency sequence of different polarity pulses with steep front. It cases wave processes in the cable and consequently to overvoltage on the stator windings of the induction motor.

It is proposed to use 6-step voltage source inverter with switches control law of 180 degrees to solve the above problem. However, such drive has satisfactory indicators of electromagnetic and electromechanical compatibility, in particular, the presence of the 6^{th} harmonic on the electromagnetic torque of the motor and the 6^{th} harmonic in the input power of inverter. This limits the speed-control range of the induction motor.

It is proposed to shift of voltage-source-inverter output voltages on 30 degrees for improving the electromagnetic and electromechanical compatibility of dual-motor induction drive. It provides by shifting the conductance of second-inverter switches.

The mathematical model based on the method of average voltages in integration step has been developed to analyze the electromechanical processes of the dual-motor electric drive with two 6-step voltage inverters which voltages are shifted by 30 degrees.

Research results proofed that proposed solution enables to improve electromagnetic compatibility of electric drive with DC source and electromechanical compatibility of electric drive with load in comparison with the individual drive, in particular to eliminate the 6th harmonic of input power of inverters and the 6th harmonic of induction-motor electromagnetic torque, to reduce pulsation amplitude of electromagnetic torque more than 8 times and more than 2 times pulsation-amplitude of input current.

Key words: dual-motor induction drive; frequency-regulated drive; electromagnetic compatibility; electromechanical compatibility

Introduction

Multi-motor induction frequency-regulated electric drives are used as an alternative to single-motor electric drives in case where there are difficulties in implementing an individual drive which are associated with the mechanical-transmission implementation. Such drives provide movement of electric vehicles, conveyors, metal rolling mills, traction units. The use of multi-motor electric drives in electric transport provides better traction of the vehicle with the road surface, a simpler mechanical transmission system [1-4].

Analysis of recent researches and publications. Problem description

Usually, two induction three-phase or multi-phase frequency-regulated induction motors are used as a multi-motor electric drive. These induction motors are applied from one or two voltage source inverters. The advantage of the using one three-phase voltage source inverter to apply two three-phase induction frequency-regulated motors is a simpler power system, which provides smaller dimensions and cost of the system [1–6]. Schematic solutions for using two three-phase voltage source inverters for applying two three-phase induction motors are known [7–9]. Such solutions are used for electric cars. In addition, it is proposed solutions for using one five-phase voltage source inverter for frequency control of two three-phase induction motors [10, 11]. In this case, one phase of each motor is connected to a common output of the inverter. The advantage of such a solution is a reduction of the semiconductor-switches number and switching losses, respectively, an increase in the efficiency of the five-phase inverter and the electric drive compared to the use of two three-phase voltage inverters [11].

In addition, dual-motor drives with one six-phase voltage source inverter are also known. Two six-phase motors are connected to output of six-phase voltage source inverter. Such solutions provide high energy characteristics (reduction of motor-torque pulsations and input current of inverter) and high fault tolerance [12–14].

It should be noted that voltage source inverter with pulse width modulation (PWM) is used as a voltage inverter in the above-described solutions. The key disadvantage of such a voltage source inverter is that the alternating voltage is formed as a high-frequency sequence of pulses of different polarity. Moreover, these pulses have a steep front due to the use of IGBT transistors with a short switching time (0.01 μs) in voltage source inverters. The existence of a pulse signal with a steep front in the cable causes the appearance of wave processes and, accordingly, overvoltages on the stator windings of an induction motor. To reduce overvoltages in the motor windings and increase the reliability of its operation and service life, an LC filter at the output of the inverter to reduce the rate of voltage change on the motor stator windings or an RC filter on the motor terminals to reduce the wave resistance of the cable is used [15]. These methods do not allow to completely eliminate the problem of overvoltages on the stator windings of an induction motor. In addition, the pulsed nature of the power supply voltage creates a number of additional problems that shorten the life of the motor, in particular: inducing voltage on the motor casing; the flow of currents through the shaft and bearings, which leads to the destruction of the bearings; flow of currents through screens of power cables; accelerated aging of insulation; emission of electromagnetic disturbances [16].

An alternative way to solve this problem is the use of three-phase voltage source inverters with a different switch operation law, in particular 6-step voltage source inverter with switches control law of 180 degrees. The 5th and 7th harmonics in the motor currents and the 6th harmonic in the electromagnetic torque and the input power of the voltage inverter appear in case of using 6-step voltage source inverter for the frequency control of an induction motor. It limits the speed-regulation ratio of induction motor. And, accordingly, it worsens the energy and electromechanical indicators of such a frequency-regulated electric drive.

Therefore, developing a schematic solution of a dual-motor frequency-controlled induction electric drive using 6-step voltage source inverters in order to improve its electromagnetic and electromechanical compatibility, analysis of the energy characteristics and electromechanical characteristics of the proposed solution by the method of mathematical modeling, is actual task.

Definition of goals and tasks of article

The presented in the article research purpose is to develop a schematic solution of a dual-motor frequency-controlled induction electric drive using two 6-step voltage source inverters in order to improve its electromagnetic and electromechanical compatibility, to develop a mathematical model of the proposed dual-motor electric drive, to analyze energy characteristics and electromechanical characteristics using a mathematical model.

Main matter description

The proposed dual-motor frequency-regulated electric drive consists of two induction motors IM1 and IM2, which shafts are mechanically connected to the working body WB. The stator windings of induction motors are applied from two 6-step voltage source inverters VSI1 and VSI2 (Fig. 1). The output voltages of inverters are shifted in time by 30 electrical degrees. The voltage inverters are connected at the input to the DC voltage source Ud.

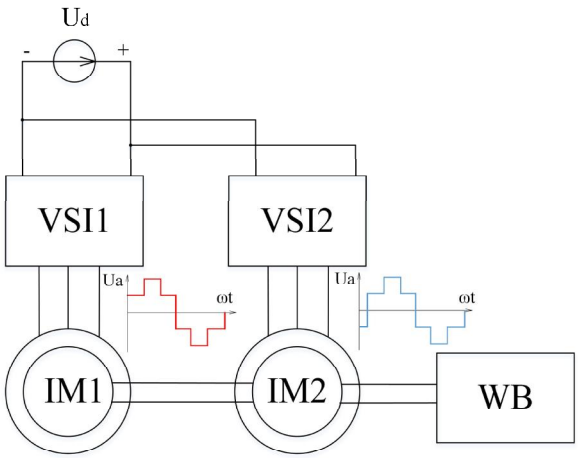

Fig. 1. Block diagram of dual-motor frequency-controlled induction drive

A mathematical model of the dual-motor frequency-controlled induction drive with two 6-step voltage source inverters was developed using the method of average voltages in integration step [17] to analyze the energy and electromechanical characteristics of system. The calculation scheme of the mathematical model is shown in Fig. 2. The mathematical model of a dual-motor frequency-controlled induction drive consists of models of system elements: an induction machine, switch groups of inverters, RL-branch with electromotive force.

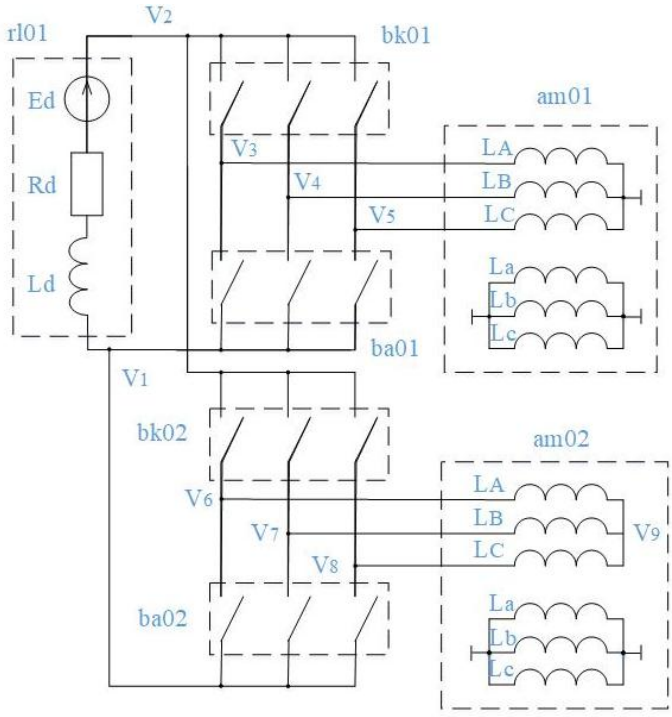

Fig. 2. Mathematical-model calculation scheme of dual-motor frequency-controlled induction drive

Method and IM-model description

The mathematical model of the dual-motor frequency-controlled induction drive according to the method of average voltages in integration step [17] is represented by a system of algebraic equations. These equations are based on the equation for an electric circuit containing electromotive force, active resistance, inductive and capacitive resistance:

$$\frac{1}{\Delta t}\int_{t_0}^{t_0+\Delta t}\left(u+e-u_R-u_C-u_L\right)dt=0. \tag{1}$$

where u, e, u_R, u_C, u_L – essential values of branch notes voltage, electromotive force, voltage on active resistance, voltage on capacitive resistance, voltage on inductive resistance, t_0 – value of time at begging of integration step, Δt – integration step.

Essential values of voltages on active resistance and capacitive resistance are represented with formulas:

$$u_{R1}=u_{R0}+\Delta u_R,\ u_{C1}=u_{C0}+\Delta u_C, \tag{2}$$

where u_{R0}, u_{C0} – value of voltage at begging of integration step; Δu_R, Δu_C – voltage increments in integration step are represented as:

$$\Delta u_R=\sum_{k=1}^{\infty}\frac{d^{(k)}u_{R0}}{dt^{(k)}}\times\frac{\left(t-t_0\right)^k}{k!},\ \Delta u_C=\sum_{k=1}^{\infty}\frac{d^{(k)}u_{C0}}{dt^{(k)}}\times\frac{\left(t-t_0\right)^k}{k!}, \tag{3}$$

where $\frac{d^{(k)}u_{R0}}{dt^{(k)}}$, $\frac{d^{(k)}u_{C0}}{dt^{(k)}}$ – k-th time derivatives of the voltages on the active resistance and the capacitor at the beginning of the step.

An equation is obtained taking into account the known dependencies between the voltages and currents of the branch elements, based on (1–3). Unknowns of this equation (4) are the branch current at the end of the integration step i_1 and the branch average voltage U in the integration step.

$$\left(\frac{R}{m+1}+\frac{\Delta t}{C}\times\frac{2-(m+1)(m+2)}{2(m+1)(m+2)}+\frac{L_0}{\Delta t}\right)i_0-\sum_{k=1}^{m-1}\left(\frac{R\Delta t^k}{(k+1)!}\times\frac{m-k}{m+1}+\frac{\Delta t^{k+1}}{C(k+2)!}\times\frac{(m+1)(m+2)-(k+1)(k+2)}{(m+1)(m+2)}\right)\frac{d^{(k)}i_0}{dt^{(k)}}+$$

$$+U+E-u_{R0}-u_{C0}-\left(\frac{R}{m+1}+\frac{\Delta t}{C(m+1)(m+2)}+\frac{L_1}{\Delta t}\right)i_1=0\,, \tag{4}$$

where i_0 – branch currents at the begging of integration step; L_0, L_1 – branch inductances at the begging and end of integration step, m – order of the polynomial that describes the current curve in the integration step (order of the method); $U=\frac{1}{\Delta t}\int_{t_0}^{t_0+\Delta t}u\,dt$, $E=\frac{1}{\Delta t}\int_{t_0}^{t_0+\Delta t}e\,dt$ − branch average voltages in integration step and electromotive force.

Each power-scheme element of dual-motor electric drive is represented as multipole and is described by vector equation (5) of the form formed on the basis of equation (4).

$$\vec{i}_e+\mathbf{G}_{se}\frac{1}{\Delta t}\int_{t_0}^{t_0+\Delta t}\vec{v}_e\,dt+\vec{C}_{se}=0\,, \tag{5}$$

where $\vec{v}_e$ – the vector of the multipole external-poles potentials; $\vec{i}_e$ – the vector of multipole external-branch currents; $\mathbf{G}_{se}$, $\vec{C}_{se}$ – matrix of coefficients and right-hand side vector.

According to Kirchoff's law equation is written:

$$\sum_{j=1}^{L}\mathbf{\Pi}_j\vec{i}_{ej}=0\,, \tag{6}$$

where $\mathbf{\Pi}_j$ – the incidence matrix of the j-th structural element, which determines the method of connecting the external branches of the multipole (element) to independent nodes of the electrical circuit; L is the number of structural elements in the power scheme. The incidence matrix establishes a relationship between the potential vector of the poles of the multipole and the potential vector of the independent nodes of the power circuit. This relationship for the average values of the potentials is described by the dependence:

$$\cdot\frac{1}{\Delta t}\int_{t_0}^{t_0+\Delta t}\vec{v}_e\,dt=\mathbf{\Pi}_e^T\frac{1}{\Delta t}\int_{t_0}^{t_0+\Delta t}\vec{v}_c\,dt\,.. \tag{7}$$

From (5), (6), (7) the following algebraic equation is obtained for the average values of the potentials of independent nodes of the system in the integration step $\frac{1}{\Delta t}\int_{t_0}^{t_0+\Delta t}\vec{v}_c\,dt$:

$$\mathbf{G}_{sc}\frac{1}{\Delta t}\int_{t_0}^{t_0+\Delta t}\vec{v}_c\,dt+\vec{C}_{sc}=0\,, \tag{8}$$

the coefficients of equation are determined on the basis of the coefficients of the vector equations (5) of all the elements included in the system (quantity L) and their incidence matrices according to the formulas:

$$\mathbf{G}_{sc}=\sum_{j=1}^{L}\mathbf{\Pi}_j\mathbf{G}_{sej}\mathbf{\Pi}_j^T,\ \vec{C}_{sc}=\sum_{j=1}^{L}\mathbf{\Pi}_j\vec{C}_{sej}\,.$$

Average values of independent-nodes potentials in the integration step are determined from equation (8). Next, average pole potential values in the integration step for each structural element are determined from equation (7) using the known incidence matrices. Currents of the external circuits at the end of the numerical integration step from equation (5)

The calculation scheme of induction machine as a 12-pole switch is presented in Fig. 3 and consists of a three-phase stator and rotor winding. In Fig. 3 it is marked $\left(v_{A1},v_{B1},v_{C1},v_{a1},v_{b1},v_{c1}\right)^T=\vec{v}_{am}^{\,I}$,

$\left(v_{A2}, v_{B2}, v_{C2}, v_{a2}, v_{b2}, v_{c2}\right)^T = \vec{v}_{am}^{II}$ – potential vectors of external poles, $\left(i_A, i_B, i_C, i_a, i_b, i_c\right)^T = \vec{i}_{am}$ – current vector of the stator and rotor windings.

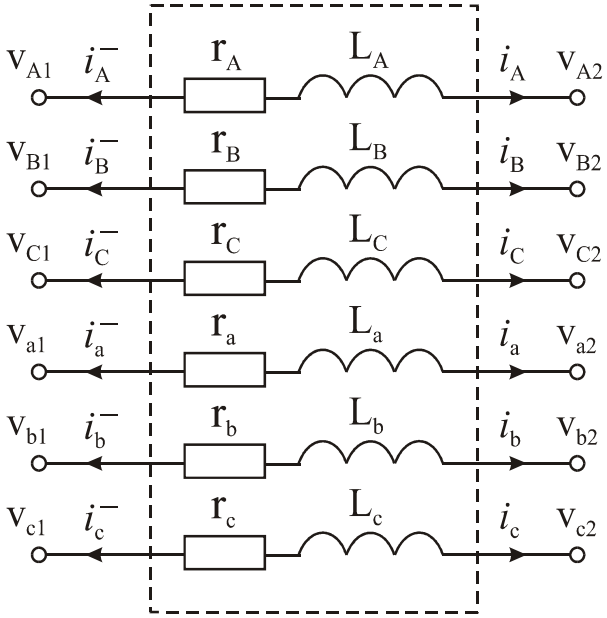

Fig. 3. Calculation scheme of induction machine

Vector equation for stator and rotor windings is written applying equation (4) for the second-order (m = 2) method of average voltage in integration step to the calculation scheme in Fig. 3:

$$\vec{U} - \vec{u}_{R0} + \frac{\mathbf{R}_{am}}{3}\vec{i}_{am0} - \frac{\mathbf{R}_{am}\Delta t}{6}\frac{d\vec{i}_{am0}}{dt} - \frac{\mathbf{R}_{am}}{3}\vec{i}_{am1} - \frac{1}{\Delta t}\left(\vec{\psi}_{am1} - \vec{\psi}_{am0}\right) = 0, \tag{8a}$$

where $\vec{U}$ - vector of average phase voltages in integration step:

$$\vec{U} = \frac{1}{\Delta t}\int_{t_0}^{t_0+\Delta t}\vec{v}_{am}^{I}\,dt - \int_{t_0}^{t_0+\Delta t}\vec{v}_{am}^{II}\,dt \quad , \tag{9}$$

$\vec{u}_{R0}$ – voltage vector on active resistance of stator and rotor windings at the beginning of integration step; $\mathbf{R}_{am} = diag\left(R_A, R_B, R_C, R_a, R_b, R_c\right)$ - matrix of active resistance; $\vec{i}_{am0}$, $\vec{i}_{am1}$ – vectors of currents at the beginning and end of integration step; $\vec{\psi}_{am0}$, $\vec{\psi}_{am1}$ – vectors of flux linkages at the beginning and end of integration step which are determined as:

$$\vec{\psi}_{am0} = \mathbf{L}_{am0}\vec{i}_{am0}, \; \vec{\psi}_{am1} = \mathbf{L}_{am1}\vec{i}_{am1}, \tag{10}$$

where $\mathbf{L}_{am0}$, $\mathbf{L}_{am1}$ – matrix of inductances at the beginning and end of integration step, diagonal elements of this matrix are self inductances, other elements are mutual inductances that depend on the rotation angle of motor.

Applying equations (8a), (9), (10) and taking into account that $\vec{u}_{R0} = \mathbf{R}_{am}\vec{i}_{am0}$, equation is written as:

$$\frac{1}{\Delta t}\int_{t_0}^{t_0+\Delta t}\vec{v}_{am}^{I}\,dt - \frac{1}{\Delta t}\int_{t_0}^{t_0+\Delta t}\vec{v}_{am}^{II}\,dt - \left(\frac{\mathbf{R}_{am}}{3} + \frac{\mathbf{L}_{am1}}{\Delta t}\right)\vec{i}_{am1} - \left(2\frac{\mathbf{R}_{am}}{3} - \frac{\mathbf{L}_{am0}}{\Delta t}\right)\vec{i}_{am0} - \frac{\mathbf{R}_{am}\Delta t}{6}\frac{d\vec{i}_{am0}}{dt} = 0. \tag{11}$$

Applying equations (11) equation for describing induction machine as multipole is written as:

$$\vec{i}_M + \mathbf{G}_M\frac{1}{\Delta t}\int_{t_0}^{t_0+\Delta t}\vec{v}_M\,dt + \vec{C}_M = 0, \tag{12}$$

where $\vec{i}_M = \begin{bmatrix} -\vec{i}_{am1} \\ \vec{i}_{am1} \end{bmatrix}$ – vector of external-branch currents, $\vec{v}_M = \begin{bmatrix} \vec{v}_{am}^{I} \\ \vec{v}_{am}^{II} \end{bmatrix}$ – vector of external poles, matrix coefficients: $\mathbf{G}_M = \begin{bmatrix} \mathbf{R}_M^{-1} & -\mathbf{R}_M^{-1} \\ -\mathbf{R}_M^{-1} & \mathbf{R}_M^{-1} \end{bmatrix}$, $\mathbf{R}_M = \frac{\mathbf{R}_{am}}{3} + \frac{\mathbf{L}_{am1}}{\Delta t}$,

$$\vec{C}_M = \begin{bmatrix} -\mathbf{R}_M^{-1}\left(2\frac{\mathbf{R}_{am}}{3} - \frac{\mathbf{L}_{am0}}{\Delta t}\right)\vec{i}_{am0} + \frac{\mathbf{R}_{am}\Delta t}{6}\frac{d\vec{i}_{am0}}{dt} \\ \mathbf{R}_M^{-1}\left(2\frac{\mathbf{R}_{am}}{3} - \frac{\mathbf{L}_{am0}}{\Delta t}\right)\vec{i}_{am0} + \frac{\mathbf{R}_{am}\Delta t}{6}\frac{d\vec{i}_{am0}}{dt} \end{bmatrix}.$$

Equation (12) is supplemented by the equation of motion:

$$J\frac{d\omega}{dt} = M - M_L, \tag{13}$$

where M – electromagnetic torque; M_L – load torque; J – total moment of inertia; ω – angular velocity.

Similar to the mathematical model of the induction machine, mathematical models of other elements are formed as multipoles [18]. Inverter switches are modeled as serially connected active and inductive resistances with variable parameters. In the case of switch turn-on, parameters of the RL branch are correspond to parameters of switch ON state, in the case switch turn-off the parameters of the RL branch are correspond to the parameters of switch OFF state.

The shift between the output voltages of the 6-step voltage source inverters is provided by shifting the conductance of the second-inverter switches by 30 electrical degrees.

Research results

The study of dual-motor frequency-controlled induction drive was carried out in the mode of frequency starting of induction dual-motors with a nominal load torque (Fig. 4–8). Nominal parameters of induction motors are given in Table 1.

Table 1

Induction motor parameters

Parameters	Values
Power, P	110 KW
Supply frequency, f	50 HZ
Number of pole pairs, p_0	4
Stator resistance, r_S	0.04 Ω
Rotor resistance, r_r	0.04 Ω
Stator leakage inductance, L_{ss}	0.00025 H
Rotor leakage inductance, L_{sr}	0.00025 H
Magnetizing inductance, L_m	0.011 H
Moment of inertia, J	2 Kgm^2

The stator-voltage effective value of the induction motors and their frequency increased linearly to the nominal values within 1.2 s during the frequency start of motors (Fig. 4, *a*). The maximum values of the stator currents during the frequency start were 2.35 times higher than the nominal values (Fig. 4, *b*).

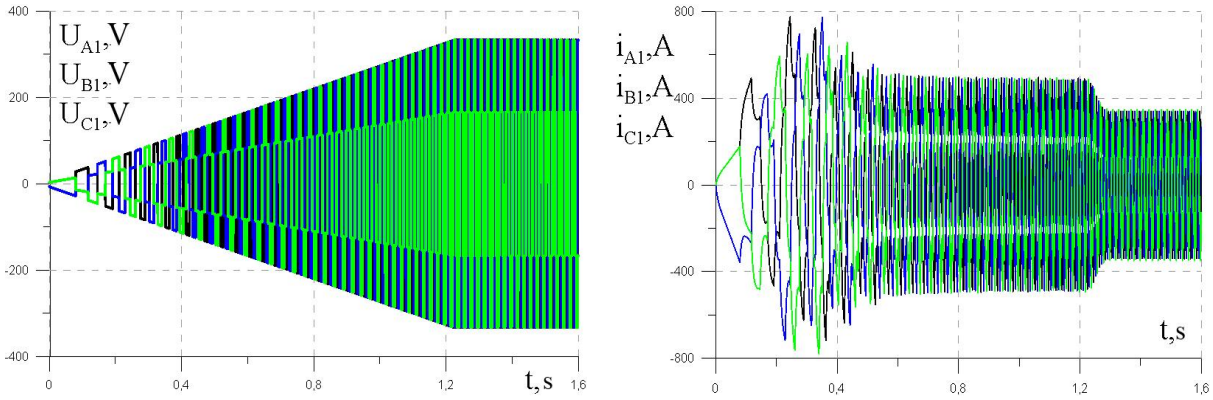

a *b*

Fig. 4. Stator phase voltages (a) and phase currents of first induction motor during frequency start

The rotation speed of the induction motors of the frequency-controlled electric drive increased to the nominal value in 1.25 s (Fig. 5, *a*), which is determined by the moment of inertia of the mechanism, while the maximum value of the electromagnetic moment exceeded the nominal value by 2.07 times. There are no starting pulse vibrations of the electromagnetic torque which are inherent for the direct start of induction motors (Fig. 5, *b*).

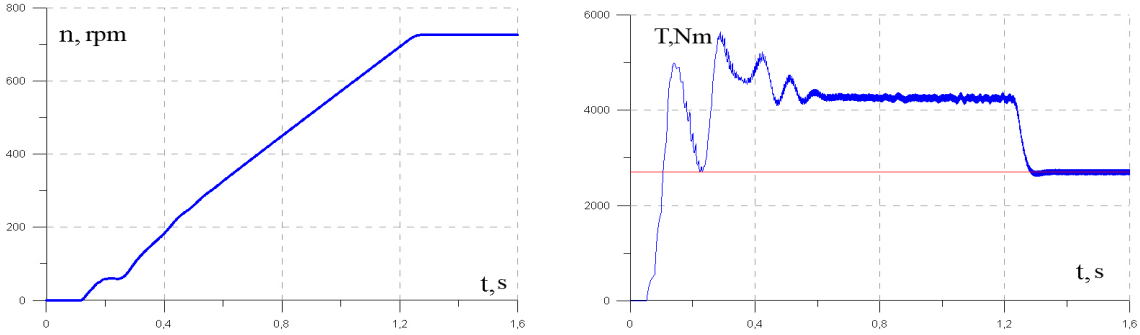

a *b*

Fig. 5. Rotation speed (a) and electromagnetic torque (b) of the induction motor during frequency start

The use of three-phase 6-step voltage source inverter with switches control law of 180 degrees provides a stepped voltage, which eliminates the problem of overvoltages on the stator windings of motors in the case of using an voltage source inverter with PWM. The output voltages of two 6-step voltage source inverters in the proposed solution of the two-motor frequency-regulated electric drive are shifted in time by 30 electrical degrees (Fig. 6).

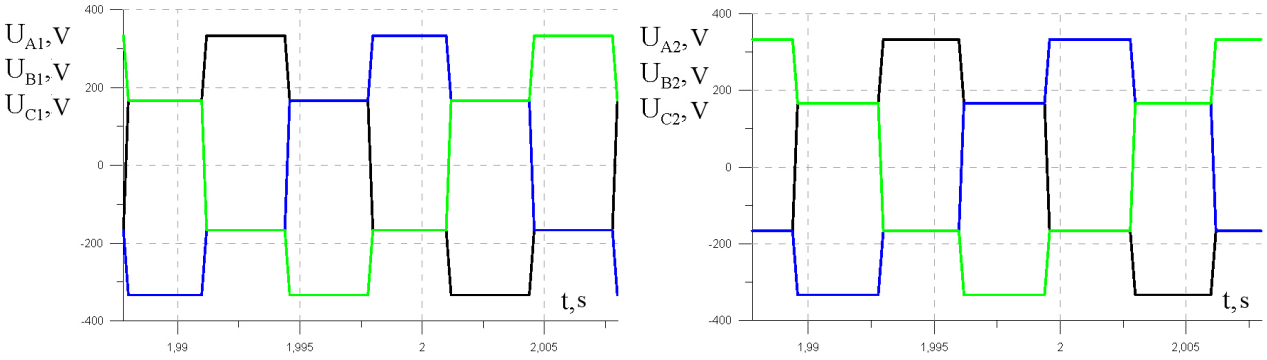

a *b*

Fig. 6. Stator phase voltage of first (a) and second (b) induction motors

The proposed solution is able to improve the electromechanical compatibility of the induction electric drive with the load. In particular, to eliminate the 6th harmonic in the electromagnetic torque (Fig. 7, *a*) in comparison with a single-motor induction electric drive (Fig. 7, *b*), and reduce the amplitude of electromagnetic–torque pulsations by more than 8 times (Table 2).

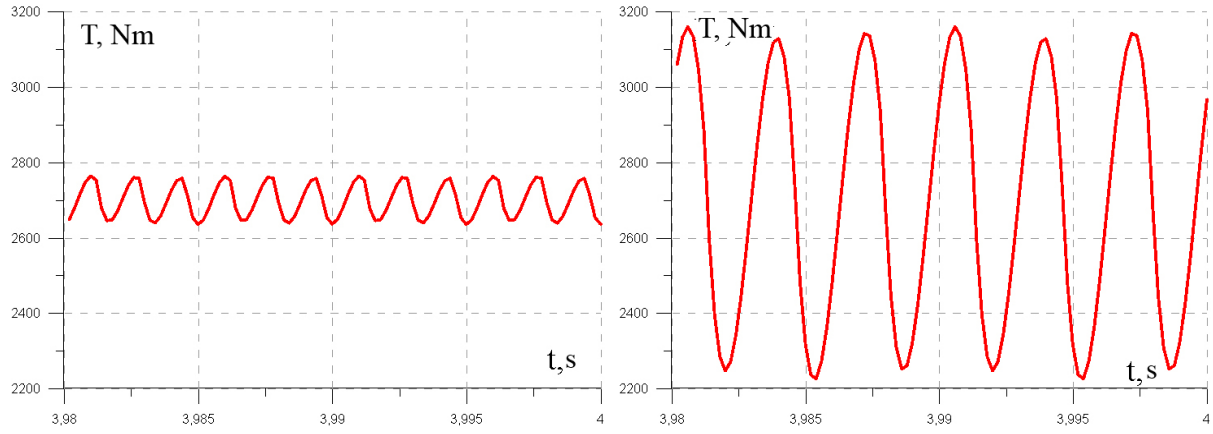

Fig. 7. Electromagnetic torque of dual-motor (a) and single-motor induction electric drive

In addition, the proposed solution is able to improve the electromagnetic compatibility of an induction electric drive with a DC voltage source. In particular eliminate the 6th harmonic in the input current (Fig. 8, *a*) of dual-motor drive in comparison with a single-motor drive (Fig. 8, *b*), and reduce the amplitude of DC source current ripples by more than 2 times (Table 2).

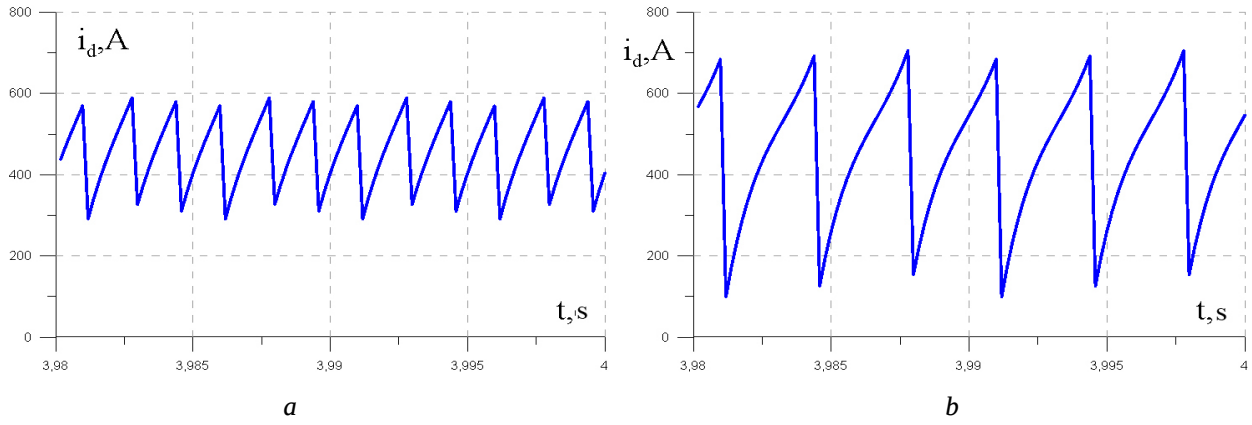

Fig. 8. Input current of the dual-motor (a) and single-motor (b) induction drive

Table 2

Indicators of electromagnetic and electromechanical compatibility of single-motor and dual-motor induction drives

No.	Indicator	Single-motor induction drive	Dual-motor induction drive
1	Type of voltage source inverter	6-Step	6-Step
2	Number of input current pulsations for period	6	12
3	Amplitude of input current pulsations, p.u.	1.5	0.65
4	Number of electromagnetic torque pulsations for period	6	12
5	Amplitude of electromagnetic torque pulsations, p.u.	0.33	0.04

Conclusions

1. The use of the dual-motor frequency-regulated induction electric drive allows solving the problems of the difficulty of mechanical-transmission implementing in single-motor electric drives of trams and locomotives trolleys where it is necessary to ensure the minimum overall dimensions of the mechanical transmission.

2. The use of 6-step voltage source inverters for frequency regulation of the induction electric drive allows to eliminate a number of problems associated with the pulsed nature of the motor supply voltage in the case of using voltage source inverters with PWM, in particular: overvoltage on the stator windings of induction motors caused by wave processes in the cable; inducing voltage on the motor casing; the flow of currents through the shaft and bearings, which leads to the destruction of the bearings; flow of currents through screens of power cables; accelerated aging of insulation; emission of electromagnetic disturbances. At the same time, the use of 6-step inverters requires the circuit solutions to improve the electromechanical and electromagnetic compatibility of the electric drive by eliminating higher harmonics in the electromagnetic torque of the motor and in the currents of the motor and power DC source.

3. The results of mathematical modeling using the mathematical model created by the method of average voltages in integration step demonstrated that the proposed solution of the dual-motor frequency-regulated induction electric drive by shifting the output voltages of 6-step voltage source inverters by 30 electric degrees is able to improve the electromagnetic and electromechanical compatibility of the electric drive in comparison with a single-motor electric drive. In particular to eliminate the 6^{th} harmonic of the input power (DC source current) and in the electromagnetic torque, to reduce the pulsation amplitude of the electromagnetic torque by 8.25 times and by 2.3 times the pulsation amplitude of the DC current.

References

1. Bouscayrol A. et al. "Multi-machine multi-converter system for drives: analysis of coupling by a global modeling", Conference Record of the 2000 IEEE Industry Applications Conference. Thirty-Fifth IAS Annual Meeting and World Conference on Industrial Applications of Electrical Energy (Cat. No.00CH37129), 2000, Vol. 3, pp. 1474–1481. DOI: 10.1109/IAS.2000.882078.

2. Joshi, B. M., Chandorkar, M. C. Two-motor single-inverter field-oriented induction machine drive dynamic performance. Sadhana 39, 2014. pp. 391–407. DOI: 10.1007/s12046-014-0237-6.

3. Gunabalan R., Sanjeevikumar P., Blaabjerg Frede, Wheeler Patrick W., Olorunfemi Ojo, and Ahmet H. Ertas. Speed sensorless vector control of parallel-connected three-phase two-motor single-inverter drive system. FACETS. 1():12 April 2016, pp. 1–16, DOI: 10.1139/facets-2015-0004

4. Bouscayrol A., Pietrzak-David M., Delarue P., Pena-Eguiluz R., Vidal P. and Kestelyn X. "Weighted Control of Traction Drives With Parallel-Connected AC Machines", in IEEE Transactions on Industrial Electronics, vol. 53, no. 6, pp. 1799–1806, Dec. 2006. DOI: 10.1109/TIE.2006.885106.

5. Ma J. D., Wu Bin, Zargari N. R. and Rizzo S. C. "A space vector modulated CSI-based AC drive for multimotor applications", in IEEE Transactions on Power Electronics, Vol. 16, No. 4, pp. 535–544, July 2001. DOI: 10.1109/63.931075.

6. Olivera V. de, Monmasson E. and Louis J. P. "Analysis of an electrical differential realized by two connected induction motors", Proc. ICEM, pp. 1862–1865, Aug. 2000.

7. Ruan J. and Song Q. "A Novel Dual-Motor Two-Speed Direct Drive Battery Electric Vehicle Drivetrain", in IEEE Access, Vol. 7, pp. 54330–54342, 2019. DOI: 10.1109/ACCESS.2019.2912994.

8. Dhote V. P. , Lokhande M. M., Agrawal A. and Kumar B. H. "Mechanical coupling of two induction motor drives for the applications of an electric-drive vehicle system", 2017 National Power Electronics Conference (NPEC), pp. 330–333. DOI: 10.1109/NPEC.2017.8310480.

9. Nayak Roopa and Pallavi Andhe, "Novel V/f Strategy Using Command Speed Compensator for Improved Load Sharing With Dual Induction Motor", International Journal of Innovative Science, Engineering & Technology, Vol. 3 Is. 2, February 2016, pp. 465–470.

10. Sabarad J., Kulkarni G. H. and Sattigeri S. "Dual three phase induction motor control using Five Leg Inverter", 2017 International Conference on Smart grids, Power and Advanced Control Engineering (ICSPACE), 2017, pp. 120–125. DOI: 10.1109/ICSPACE.2017.8343416.

11. Kellner Jakub, Praženica Michal, Two five-phase induction motors used as an electronic differential, Transportation Research Procedia, Vol. 55, 2021, pp. 896–903, ISSN 2352-1465. DOI: 10.1016/j.trpro.2021.07.058.

12. Lim Y. -S., Lee J. -S. and Lee K. -B. "Advanced Speed Control for a Five-Leg Inverter Driving a Dual-Induction Motor System", in IEEE Transactions on Industrial Electronics, Vol. 66, No. 1, pp. 707–716, Jan. 2019. DOI: 10.1109/TIE.2018.2831172.

13. Levi, E., Jones, M., Vukosavic, S. N. and Toliyat, H. A., A novel concept of a multiphase, multimotor vector controlled drive system supplied from a single voltage source inverter. In IEEE Transactions on Power Electronics, Vol. 19, No. 2, pp. 320–335, March 2004. DOI: 10.1109/TPEL.2003.823241.

14. Levi E., M. Jones, Vukosavic, S.N. and Toliyat, H.A., 2004. A Five-Phase Two-Machine Vector Controlled Induction Moto Drive Supplied from a Single Inverter. In EPE Journal, 14:3, pp. 38–48. DOI: 10.1080/09398368.2004.11463564.

15. Kazachkovskyi M. M. Avtonomni peretvoriuvachi ta peretvoriuvachi chastoty: navchalnyi posibnyk/ Dnipropetrovsk: NHA Ukrainy, 2000. 197 s.

16. Zientek P. Wpływ parametrów wyjciowych falownikĄw pwm i kabla zasilajcego na zjawiska pasoytnicze w silnikach indukcyjnych (Influence of the pwm inverters output parameters and power cable on the additional phenomena occuring in induction motors). Zeszyty Problemowe – Maszyny Elektryczne, Nr 71/2005, pp. 119–124.

17. Plakhtyna O., Kutsyk A., Semeniuk M. Real-Time Models of Electromechanical Power Systems, Based on the Method of Average Voltages in Integration Step and Their Computer Application. Energies 2020, 13, *2263. https://doi.org/10.3390/en13092263.*

18. Kutsyk A. A Real-Time Model of Locomotion Module DTC Drive for Hardware-In-The-Loop Implementation. Retrieved from https://par.nsf.gov/biblio/10316670. PRZEGLĄD ELEKTROTECHNICZNY 1.6 Web. DOI:10.15199/48.2021.06.11.

Список літератури

1. Bouscayrol A. et al. "Multi-machine multi-converter system for drives: analysis of coupling by a global modeling", Conference Record of the 2000 IEEE Industry Applications Conference. Thirty-Fifth IAS Annual Meeting and World Conference on Industrial Applications of Electrical Energy (Cat. No.00CH37129), 2000, Vol. 3, pp. 1474–1481. DOI: 10.1109/IAS.2000.882078.

2. Joshi B. M., Chandorkar M. C. Two-motor single-inverter field-oriented induction machine drive dynamic performance. Sadhana 39, 2014, pp. 391–407. DOI: 10.1007/s12046-014-0237-6.

3. Gunabalan R., Sanjeevikumar P., Blaabjerg F., Patrick W. Wheeler, Olorunfemi Ojo, and Ahmet H. Ertas. Speed sensorless vector control of parallel-connected three-phase two-motor single-inverter drive system. FACETS. 1():12 April 2016, pp. 1–16. 10.1139/facets-2015-0004

4. Bouscayrol A., Pietrzak-David M., Delarue P., Pena-Eguiluz R., Vidal P. and Kestelyn X. "Weighted Control of Traction Drives With Parallel-Connected AC Machines", in IEEE Transactions on Industrial Electronics, Vol. 53, No. 6, pp. 1799–1806, Dec. 2006. DOI: 10.1109/TIE.2006.885106.

5. Ma J. D., Wu Bin, Zargari N. R. and Rizzo S. C. "A space vector modulated CSI-based AC drive for multimotor applications", in IEEE Transactions on Power Electronics, Vol. 16, No. 4, pp. 535–544, July 2001. DOI: 10.1109/63.931075.

6. Olivera V. de, E. Monmasson and Louis J. P. "Analysis of an electrical differential realized by two connected induction motors", Proc. ICEM, pp. 1862–1865, Aug. 2000.

7. Ruan J. and Song Q. "A Novel Dual-Motor Two-Speed Direct Drive Battery Electric Vehicle Drivetrain", in IEEE Access, Vol. 7, pp. 54330–54342, 2019. DOI: 10.1109/ACCESS.2019.2912994.

8. Dhote V. P., Lokhande M. M., Agrawal A. and Kumar B. H. "Mechanical coupling of two induction motor drives for the applications of an electric-drive vehicle system", 2017 National Power Electronics Conference (NPEC), 2017, pp. 330–333. DOI: 10.1109/NPEC.2017.8310480.

9. Roopa Nayak and Andhe Pallavi "Novel V/f Strategy Using Command Speed Compensator for Improved Load Sharing With Dual Induction Motor", International Journal of Innovative Science, Engineering & Technology, Vol. 3, Is. 2, February 2016, pp. 465–470.

10. Sabarad J., Kulkarni G. H. and Sattigeri S. "Dual three phase induction motor control using Five Leg Inverter", 2017 International Conference on Smart grids, Power and Advanced Control Engineering (ICSPACE), 2017, pp. 120–125. DOI: 10.1109/ICSPACE.2017.8343416.

11. Jakub Kellner, Michal Praženica, Two five-phase induction motors used as an electronic differential, Transportation Research Procedia, Vol. 55, 2021, pp. 896–903. ISSN 2352-1465. DOI: 10.1016/j.trpro.2021.07.058.

12. Lim Y.-S., Lee J.-S. and Lee K.-B. "Advanced Speed Control for a Five-Leg Inverter Driving a Dual-Induction Motor System", in IEEE Transactions on Industrial Electronics, Vol. 66, No. 1, pp. 707–716, Jan. 2019. DOI: 10.1109/TIE.2018.2831172.

13. Levi, E., Jones, M., Vukosavic, S. N. and Toliyat, H. A., 2004. A novel concept of a multiphase, multimotor vector controlled drive system supplied from a single voltage source inverter. In IEEE Transactions on Power Electronics, Vol. 19, No. 2, pp. 320–335, March 2004. DOI: 10.1109/TPEL.2003.823241.

14. Levi E., Jones M., Vukosavic S. N. and Toliyat H. A. A Five-Phase Two-Machine Vector Controlled Induction Moto Drive Supplied from a Single Inverter. In EPE Journal, 14:3, 38–48., DOI: 10.1080/09398368.2004.11463564.

15. Казачковський М. М. Автономні перетворювачі та перетворювачі частоти: навч. посіб. Дніпропетровськ: НГА України, 2000. 197 с.

16. Zientek P. Wpływ parametrów wyjciowych falowników pwm i kabla zasilajcego na zjawiska pasoytnicze w silnikach indukcyjnych (Influence of the pwm inverters output parameters and power cable on the additional phenomena occuring in induction motors). Zeszyty Problemowe – Maszyny Elektryczne, Nr 71/2005, pp. 119–124.

17. Plakhtyna O., Kutsyk A., Semeniuk M. Real-Time Models of Electromechanical Power Systems, Based on the Method of Average Voltages in Integration Step and Their Computer Application. Energies, 2020, 13, 2263. https://doi.org/10.3390/en13092263.

18. Kutsyk A. A Real-Time Model of Locomotion Module DTC Drive for Hardware-In-The-Loop Implementation. Retrieved from https://par.nsf.gov/biblio/10316670. PRZEGLĄD ELEKTROTECHNICZNY 1.6 Web. DOI:10.15199/48.2021.06.11.

М. Б. Семенюк
Національний університет "Львівська політехніка",
кафедра електромехатроніки та комп'ютеризованих електромеханічних систем,
mykola.b.semeniuk@lpnu.ua

А. С. Куцик
Національний університет "Львівська політехніка",
кафедра електромехатроніки та комп'ютеризованих електромеханічних систем,
andrii.s.kutsyk@lpnu.ua

Гжегож Подскарбі
Політехніка Жешовська (Польща),
факультет електротехніки та інформатики

ДВОДВИГУННИЙ ЧАСТОТНОРЕГУЛЬОВАНИЙ АСИНХРОННИЙ ЕЛЕКТРОПРИВІД З ПОКРАЩЕНИМИ ЕЛЕКТРОМАГНІТНОЮ ТА ЕЛЕКТРОМЕХАНІЧНОЮ СУМІСНІСТЮ

Дводвигунний асинхронний частотнорегульований електропривід використовують як альтернативу однодвигунного електроприводу в тих випадках, коли є складності в реалізації однодвигуннного електроприводу, які зв'язані з реалізацією механічної передачі. Дводвигунний електропривід приводить в рух тягові механізми, робочі органи електротранспортних засобів. Для живлення двох асинхронних двигунів використовують один або два автономних інвертори напруги з широтно-імпульсною модуляцією. Недоліком таких інверторів напруги є те, що змінна напруга формується як високочастотна послідовність імпульсів різної полярності з крутим фронтом. Це спричиняє появу хвильових процесів у кабелі та, відповідно, перенапруги на обмотках статора асинхронного двигуна.

Для вирішення проблеми запропоновано використовувати шеститактні інвертори напруги із законом керування ключами 180 град. Проте такий привід має задовільні показники

електромагнітної та електромеханічної сумісності, зокрема, наявність шостої гармоніки в електромагнітному моменті двигуна та шостої гармоніки у вхідній потужності інвертора. Це обмежує діапазон регулювання частоти обертання асинхронного двигуна.

З метою покращення електромагнітної та електромеханічної сумісності у дводвигунному електроприводі запропоновано зміщення в часі вихідних напруг шеститактних інверторів на 30 електричних градусів, що досягається зміщенням провідності вентилів другого інвертора.

Для аналізу електромеханічних процесів дводвигунного електроприводу з двома шеститактними інверторами напруги, зміщеними в час на 30°, розроблено математичну модель методом середніх напруг на кроці числового інтегрування.

Результати математичного моделювання підтвердили, що запропоноване рішення дає змогу покращити електромагнітну сумісність електроприводу з джерелом постійної напруги та електромеханічну сумісність електроприводу з навантаження порівняно з однодвигунним електроприводом, зокрема ліквідувати шосту гармоніку вхідної потужності інверторів та шосту гармоніку електромагнітного моменту асинхронного електроприводу, зменшити більше ніж у вісім разів амплітуду пульсації електромагнітного моменту та більше ніж у два рази амплітуду пульсації вхідного струму.

Ключові слова: дводвигунний асинхронний електропривід; частотнорегульований електропривід; шеститактний інвертор напруги; математичне моделювання.